Continuously Steerable Differential Beamformers with Null Constraints for Circular Microphone Arrays

Gongping Huang,[1, a] Israel Cohen,[1, b] Jingdong Chen,[2, c] and Jacob Benesty[3, d]
[1] *Andrew and Erna Viterby Faculty of Electrical Engineering, Technion – Israel Institute of Technology, Technion City, Haifa 3200003, Israel.*
[2] *Center of Intelligent Acoustics and Immersive Communications, Northwestern Polytechnical University, Xi'an, Shaanxi 710072, China.*
[3] *INRS-EMT, University of Quebec, 800 de la Gauchetiere Ouest, Montreal, QC H5A 1K6, Canada.*

Differential beamforming combined with microphone arrays can be used in a wide range of applications related to acoustic and speech signal acquisition and recovery. A practical and useful method for designing differential beamformers is the so-called null-constrained one, which was developed based on linear arrays and requires only the nulls' information from the target directivity pattern. While it is effective and easy to use, this method is found not suitable for designing steerable differential beamformers with circular arrays. This paper reexamines this technique in the context of circular differential microphone arrays. By analyzing the properties of the circular array topology, the null-constrained method is extended to including symmetric constraints, which is inherent in the design of circular arrays. This extension yields a design method for fully steerable differential beamformers that require only minimum information from the target beampattern. Simulations justify the theoretical analysis and demonstrate the good properties of the developed method.

 [https://doi.org(DOI number)]

[XYZ] Pages: 1–10

PACS numbers: 43.72.Dv 43.60.Fg

I. INTRODUCTION

Array beamforming, which aims at recovering a signal of interest from noisy observations with a spatial filter, has been used in a wide range of applications such as sonar, radar, speech communication, and human-machine speech interfaces (Benesty and Chen, 2012; Benesty *et al.*, 2017; Bitzer and Simmer, 2001; Crocco and Trucco, 2010; Elko and Meyer, 2008; Yan *et al.*, 2007). Intensive efforts have been devoted to this topic (Bouchard *et al.*, 2009; Gannot *et al.*, 2004; Schwartz *et al.*, 2017; Yan *et al.*, 2011). While the fundamental theory stays the same, the design of arrays and the associated beamforming algorithms vary significantly for different applications. For example, in most sonar and radar systems, the signals of interest are narrowband. In such scenarios, the array is generally designed with a half-wavelength spacing and the associated beamforming is achieved by the principle of coherently adding (i.e., compensating) the time delays according to the time-difference-of-arrival (TDOA) information so that the desired signal components from different sensors are synchronized and then adding the delay-compensated signals together. However, such a design does not work well with speech applications, where the signals of interest are wideband in nature (their frequencies generally span from approximately 20 Hz to 20 kHz), and the geometry, aperture, and the number of sensors of the array are often limited by many practical factors such as the size of the host devices, the positions to mount the sensors, and the restrictions on the cost and complexity, etc. Consequently, how to design broadband beamformers that can achieve high spatial gain and frequency-invariant spatial responses with small microphone arrays has become a critical yet challenging problem in speech applications. A significant amount of attention has been devoted to this problem. Among the many different approaches developed in the literature, the so-called differential beamforming, which makes the array responsive to the differential acoustic pressure field (the resulting array is called differential microphone array, or DMA in short) has been found particularly useful (Buchris *et al.*, 2019; Buck, 2002; Elko and Meyer, 2008; Elko and Pong, 1997; Huang *et al.*, 2020b; Kolundzija *et al.*, 2011).

Since they use finite differences between the sensors' outputs to approximate the true acoustic pressure differentials, DMAs require the sensor spacing to be much smaller than the smallest acoustic wavelength in the fre-

[a] gongpinghuang@gmail.com
[b] icohen@ee.technion.ac.il
[c] jingdongchen@ieee.org
[d] benesty@emt.inrs.ca

quency band of interest. Consequently, they are generally small in size and can be easily integrated into small or portable devices. The fundamental principle of DMAs can be traced back to the introduction of the so-called directional microphones (Olson, 1946). This principle was then used in different fields, such as the direction-finding-and-ranging (DIFAR) sensors in sonar (Greene Jr *et al.*, 2004) and microphone arrays. The earliest effort for differential beamforming in microphone arrays is the multistage DMA, in which an Nth-order DMA is formed by subtracting the outputs of two DMAs of order $N-1$ from each other (Elko, 1996, 2004). While it lays out the foundation for differential beamforming, this method lacks flexibility in forming different beampatterns and dealing with white noise amplification, which is inherent to DMAs, particularly at low frequencies. Then, a method was developed with linear arrays in the short-time Fourier transform (STFT) domain (Benesty and Chen, 2012; Chen *et al.*, 2014), where the differential beamformer is designed in each subband by solving a linear system of equations constructed from constraints on the nulls' directions of the target directivity pattern. This method is not only flexible to design beampatterns of any kind, but it can also improve the white noise gain by increasing the number of sensors while fixing the order of the DMA, leading to an optimal way in dealing with white noise amplification. Furthermore, this method uses only information about the nulls' directions. It is therefore easy to implement in practice.

Linear DMAs do not have much flexibility in terms of beam steering, and their optimal performance in terms of directivity factor (DF) occurs only at the endfire direction (Benesty and Chen, 2012). To improve the steering flexibility of differential beamformers, which is required in many applications such as teleconferencing and human-machine interfaces, circular arrays are used (Bernardini *et al.*, 2017; Borra *et al.*, 2019, 2020; Buchris *et al.*, 2020; Byun *et al.*, 2018; Huang *et al.*, 2020a; Lovatello *et al.*, 2018; Yan, 2015). However, the null-constrained method was found ineffective in the context of circular arrays. To deal with this issue, some symmetrical properties on the beamformer coefficients caused by the circular symmetry of the array geometry were considered (Benesty *et al.*, 2015). However, beamformers designed with this technique do not have full steering flexibility and the resulting beampatterns can only be perfectly steered to a few directions, i.e., the angular positions of the array elements (Benesty *et al.*, 2015; Huang *et al.*, 2017a).

An alternative way to design steerable differential beamformers is by using the series expansion method (Huang *et al.*, 2017b), which approximates the beamformer's beampattern using the Jacobi-Anger series expansion and then identifies the beamforming coefficients using the relationship between the beamformer's beampattern and the target directivity pattern (Huang *et al.*, 2018). By including the steering information in the desired directivity pattern, the designed beampattern can be flexibly steered to different directions (Huang *et al.*, 2019). However, in order to use this method, the target directivity pattern must be given as the *a priori* information, which may not be accessible in some applications.

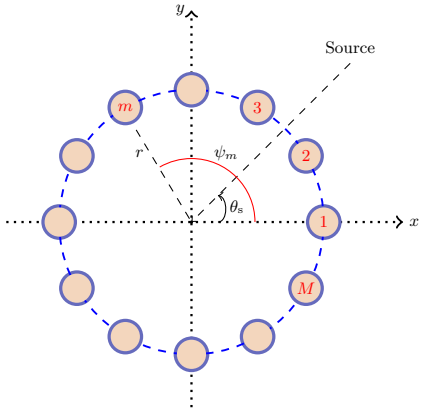

FIG. 1. Illustration of a UCA consisting of M microphones.

This paper deals with differential beamforming with circular microphone arrays. We reexamine the null-constrained method in the context of circular microphone arrays. By analyzing the properties of the circular array topology, we identify the problems with the existing techniques and develop an improved version that can design fully steerable differential beamformers. In comparison with the method presented in (Benesty *et al.*, 2015), the advantage of the developed approach is that the resulting beampattern can be steered to any direction in the sensor plane, where the change in the beampattern is only up to a rotation, i.e., the beamformer is fully steerable. Compared with the series expansion method, the developed approach only requires to know the steering and nulls' directions instead of the exact target directivity pattern, which makes it more practical in real-world applications.

The organization of this paper is as follows. Section II presents the signal model, problem formulation, and performance measures. Section III describes the desired directivity pattern as well as the conventional null-constrained method. In Section IV, we present a method to design steerable differential beamformers with symmetric null constraints. In Section V, we present some simulation results to validate the theoretical derivations. Finally, conclusions are given in VI.

II. SIGNAL MODEL, PROBLEM FORMULATION, AND PERFORMANCE MEASURES

Consider a uniform circular array (UCA) of radius r, consisting of M omnidirectional microphones. We assume that the center of the UCA coincides with the origin of the Cartesian coordinate system, azimuthal angles are measured anti-clockwise from the x axis, and Sensor 1 of the array is placed on the x axis, as illustrated in Fig. 1. The angular position of the mth array element is then $\psi_m = 2\pi(m-1)/M$, $m = 1, 2, \ldots, M$. In this scenario,

the steering vector is defined as

$$\mathbf{d}(\omega,\theta)=\left[e^{\jmath\frac{\omega r}{c}\cos(\theta-\psi_1)}\ \cdots\ e^{\jmath\frac{\omega r}{c}\cos(\theta-\psi_M)}\right]^T, \tag{1}$$

where the superscript ^{T} denotes the transpose operator, $\jmath$ is the imaginary unit with $\jmath^2=-1$, $\omega=2\pi f$ is the angular frequency, $f>0$ is the temporal frequency, and c is the speed of sound in the air (typically $c\approx 340$ m/s). The acoustic wavelength is $\lambda=c/f$. For a uniform circular array, the interelement spacing is $\delta=2r\sin(\pi/M)$. Here, we consider small array apertures, where the sensor spacing is much smaller than the acoustic wavelength.

Assume that the desired signal propagates from the direction $\theta_{\rm s}$, the received signal at the mth ($m=1,2,\ldots,M$) microphone is expressed as

$$Y_m(\omega)=e^{\jmath\frac{\omega r}{c}\cos(\theta_{\rm s}-\psi_m)}X(\omega)+V_m(\omega), \tag{2}$$

where $X(\omega)$ is the desired signal and $V_m(\omega)$ is the additive noise at the mth microphone. In a vector form, (2) becomes

$$\begin{aligned}\mathbf{y}(\omega)&=\left[\,Y_1(\omega)\ \ Y_2(\omega)\ \ \cdots\ \ Y_M(\omega)\,\right]^T\\&=\mathbf{d}(\omega,\theta_{\rm s})X(\omega)+\mathbf{v}(\omega),\end{aligned} \tag{3}$$

where $\mathbf{d}(\omega,\theta_{\rm s})$ is the signal propagation vector (same as the steering vector at $\theta_{\rm s}$) and $\mathbf{v}(\omega)$ is the noise signal vector of length M.

Beamforming aims at recovering the desired signal, $X(\omega)$, from noisy microphone observations, $\mathbf{y}(\omega)$, with a spatial filter, i.e.,

$$\begin{aligned}Z(\omega)&=\mathbf{h}^H(\omega)\mathbf{y}(\omega)\\&=\mathbf{h}^H(\omega)\mathbf{d}(\omega,\theta_{\rm s})X(\omega)+\mathbf{h}^H(\omega)\mathbf{v}(\omega),\end{aligned} \tag{4}$$

where the superscript ^{H} is the conjugate-transpose operator and $\mathbf{h}(\omega)$ is the beamforming filter of length M. In our context, the distortionless constraint is desired, i.e.,

$$\mathbf{h}^H(\omega)\mathbf{d}(\omega,\theta_{\rm s})=1. \tag{5}$$

The beampattern, which describes the sensitivity of the beamformer to a plane wave (source signal) impinging on the array from the direction θ, is defined as

$$\mathcal{B}[\mathbf{h}(\omega),\theta]=\mathbf{h}^H(\omega)\mathbf{d}(\omega,\theta). \tag{6}$$

The directivity factor (DF), which quantifies how the microphone array performs in the presence of diffuse (spherically isotropic) noise, is expressed as (Elko and Meyer, 2008)

$$\mathcal{D}[\mathbf{h}(\omega)]=\frac{\left|\mathbf{h}^H(\omega)\mathbf{d}(\omega,\theta_{\rm s})\right|^2}{\mathbf{h}^H(\omega)\mathbf{\Gamma}_{\rm d}(\omega)\mathbf{h}(\omega)}, \tag{7}$$

where $\mathbf{\Gamma}_{\rm d}(\omega)$ is the pseudo-coherence matrix of the diffuse noise, whose (i,j)th element is $[\mathbf{\Gamma}_{\rm d}(\omega)]_{ij}=\operatorname{sinc}(\omega\delta_{ij}/c)$, with $\delta_{ij}=2r\left|\sin[(i-j)\pi/M]\right|$ being the distance between microphones i and j.

Finally, the white noise gain (WNG), which evaluates the sensitivity of the array to its imperfections, is defined as (Benesty and Chen, 2012)

$$\mathcal{W}[\mathbf{h}(\omega)]=\frac{\left|\mathbf{h}^H(\omega)\mathbf{d}(\omega,\theta_{\rm s})\right|^2}{\mathbf{h}^H(\omega)\mathbf{h}(\omega)}. \tag{8}$$

III. CONVENTIONAL NULL-CONSTRAINED DIFFERENTIAL BEAMFORMING

DMAs attempt to measure the spatial derivatives of the acoustic pressure field. Early designs of DMAs are based on the uniform linear geometry and a multistage subtraction manner where the output of an Nth-order DMA is the difference between the outputs of two DMAs of order $N-1$ (Elko, 2004; Elko and Meyer, 2008). This results in a frequency-independent beampattern, which is a polynomial of $\cos\theta$ and the order of this polynomial depends on the order of the differential field to be measured, i.e., the frequency-independent directivity pattern of an Nth-order differential beamformer with the main beam pointing to the direction of 0° is

$$\mathcal{B}_N(\theta)=\sum_{n=0}^{N}a_{N,n}\cos^n\theta, \tag{9}$$

where $a_{N,n}$, $n=0,1,\ldots,N$ are real coefficients. Note that the properties of the beampattern vary with the values of the coefficients $a_{N,n}$. It is generally required that $\sum_{n=0}^{N}a_{N,n}=1$.

Given that an Nth-order differential beamformer has a beampattern of the form (9), one can also design the beamformer in an optimal way, i.e., finding the beamforming filter, $\mathbf{h}(\omega)$, such that the designed beampattern, $\mathcal{B}[\mathbf{h}(\omega),\theta]$, is equal, or as close as possible, to the target frequency-invariant beampattern, $\mathcal{B}_N(\theta)$, i.e.,

$$\mathcal{B}[\mathbf{h}(\omega),\theta]=\mathcal{B}_N(\theta),\ \forall\omega. \tag{10}$$

Let us start with a brief review of differential beamforming with linear arrays (Benesty and Chen, 2012; Chen *et al.*, 2014). The design is generally based on the fact that any ideal frequency-independent directivity pattern has a one at the endfire direction and a number of nulls in other directions and this number is uniquely determined by the order of the differential beamformer. Consequently, the DMA beamformer can be designed based on the use of the nulls' information in the range $(0,\ \pi]$, i.e., forcing the designed beampattern and the desired frequency-invariant beampattern to have the same nulls in this range. Assume that the Nth-order directivity pattern has N distinct nulls that satisfy $0<\theta_{N,1}<\cdots<\theta_{N,N}\leq\pi$, and the linear array satisfies the requirement for a DMA, then the problem of differential beamforming becomes one of solving the following linear system of equations (Benesty and Chen, 2012; Chen *et al.*, 2014):

$$\mathbf{D}(\omega)\mathbf{h}(\omega)=\mathbf{i}_{N+1}, \tag{11}$$

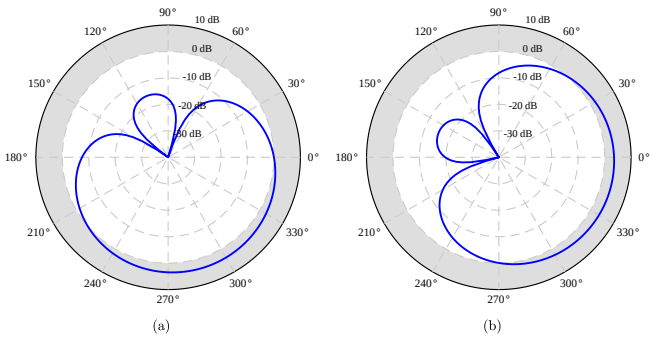

FIG. 2. Beampatterns of the differential beamformer designed directly with the conventional null-constrained method: (a) $\theta_{\mathrm{s}} = 0^{\circ}$ and (b) $\theta_{\mathrm{s}} = 50^{\circ}$. Conditions: $M = 8$, UCA with $r = 2.0$ cm, and $f = 1$ kHz.

where

$$\mathbf{D}(\omega) = \begin{bmatrix} \mathbf{d}^H(\omega, 0^{\circ}) \\ \mathbf{d}^H(\omega, \theta_{N,1}) \\ \vdots \\ \mathbf{d}^H(\omega, \theta_{N,N}) \end{bmatrix} \tag{12}$$

is a matrix of size $(N+1) \times (N+1)$, $\mathbf{d}(\omega, \theta)$ is the steering vector associated with the linear array, and $\mathbf{i}_{N+1}$ is a vector of length $N+1$, whose first element is 1 and all the other elements are 0.

To design an Nth-order linear DMA, $M \geq N+1$ microphones are needed. If this condition is satisfied, the solution to (11) is (Benesty and Chen, 2012; Chen *et al.*, 2014)

$$\mathbf{h}(\omega) = \mathbf{D}^H(\omega) \left[\mathbf{D}(\omega)\, \mathbf{D}^H(\omega)\right]^{-1} \mathbf{i}_{N+1}. \tag{13}$$

Generally, this method works well with linear arrays as demonstrated in (Benesty and Chen, 2012; Chen *et al.*, 2014), but it encounters some problems with circular arrays. To illustrate this, we present two examples in Fig. 2, where the UCA, of radius $r = 2.0$ cm, consists of eight sensors. We attempt to design a 2nd-order hypercardioid with two nulls. When $\theta_{\mathrm{s}} = 0^{\circ}$, the two nulls are at 72° and 144°. When $\theta_{\mathrm{s}} = 50^{\circ}$, the two nulls are at 122° and 194°. As seen, neither of the two cases generates legitimate beampatterns. Although they have nulls and unit gain at the specified directions, the beampatterns have gains exceeding 1 in many other directions, which may cause noise, interference, and reverberation amplification instead of reduction, which is undesirable. The underlying reason for this is due to the symmetric properties of the UCA, which are not taken into account in the beamforming process.

To circumvent this issue, Benesty et al. developed in (Benesty *et al.*, 2015) a method that considers the following symmetric property of the beampattern, i.e.,

$$\mathcal{B}[\mathbf{h}(\omega), \theta] = \mathcal{B}[\mathbf{h}(\omega), -\theta], \tag{14}$$

which leads to the following relationships in the beamforming filter:

$$H_{m+1}(\omega) = H_{M-m+1}(\omega), \tag{15}$$

where $m = 1, 2, \ldots, M - \lfloor \frac{M}{2} \rfloor - 1$, with $\lfloor \frac{M}{2} \rfloor$ stands for the integral part of $M/2$. Applying the above relationships to form the linear system of equations as in (11) can successfully resolve the design problem (Benesty *et al.*, 2015). While it is a very practical approach, which can be used to design differential beamformers by applying only nulls information, this method exhibits some limitations, i.e., the designed beampatterns can be "fully" steered only to M directions (Benesty *et al.*, 2015) ("full steering" means that the beampatterns are identical up to a rotation).

An alternative approach to the design of steerable differential beamformers is through the use of the series expansion method (Huang *et al.*, 2017b, 2018), which approximates the beamformer's beampattern using the Jacobi-Anger series expansion and then identifies the beamforming filter by forcing the approximated beampattern to be equal to the desired directivity pattern. By including the steering information, this method can successfully design the differential beamformer and fully steer the beampattern to any direction in the sensor plane. However, unlike the nulls-constrained method, this approach requires the knowledge of the target beampattern, which may not be available in practice. Therefore, there is a need to investigate and extend previous null-constrained methods to design differential beamformers for UCAs with steering flexibility, which is the focus of this paper.

IV. STEERABLE DIFFERENTIAL BEAMFORMERS BASED ON SYMMETRIC NULL CONSTRAINTS

The frequency-independent directivity pattern of an Nth-order differential beamformer corresponding to a desired steering direction, θ_{s}, can be written as

$$\mathcal{B}_{N,\theta_{\mathrm{s}}}(\theta) = \sum_{n=0}^{N} a_{N,n} \cos^n(\theta - \theta_{\mathrm{s}}). \tag{16}$$

From (16), it is seen that the frequency-independent directivity pattern, on a polar plot, is symmetric with respect to $\theta_{\mathrm{s}} \leftrightarrow (\theta_{\mathrm{s}} + \pi)$, i.e.,

$$\mathcal{B}_{N,\theta_{\mathrm{s}}}(\theta_{\mathrm{s}} + \theta') = \mathcal{B}_{N,\theta_{\mathrm{s}}}(\theta_{\mathrm{s}} - \theta'), \tag{17}$$

where $\theta' \in [0, \pi]$. Consequently, when designing a differential beamformer, the main beam should be in the direction θ_{s}, and the beampattern has to be symmetric with respect to the line $\theta_{\mathrm{s}} \leftrightarrow \theta_{\mathrm{s}} + \pi$ with $\theta \in [0, \pi]$, i.e.,

$$\mathcal{B}[\mathbf{h}(\omega), \theta_{\mathrm{s}} + \theta] = \mathcal{B}[\mathbf{h}(\omega), \theta_{\mathrm{s}} - \theta]. \tag{18}$$

Note that the beampattern of a differential beamformer designed with a linear array is always symmetric with

respect to $0 \leftrightarrow \pi$. Consequently, if $\mathcal{B}\left[\mathbf{h}\left(\omega\right), \theta_{N,n}\right] = 0$, we have $\mathcal{B}\left[\mathbf{h}\left(\omega\right), -\theta_{N,n}\right] = 0$ as well. But this is not the case for UCAs. For a differential beamformer with UCAs, $\mathcal{B}\left[\mathbf{h}\left(\omega\right), \theta_{\mathrm{s}} + \theta_{N,n}\right] = 0$ does not mean that $\mathcal{B}\left[\mathbf{h}\left(\omega\right), \theta_{\mathrm{s}} - \theta_{N,n}\right] = 0$.

Let us first consider the case where the desired directivity pattern of an Nth-order differential beamformer pointing to 0° has N distinct nulls $\theta_{N,n}$, $n = 1, 2, \ldots, N$, with $0 < \theta_{N,1} < \cdots < \theta_{N,N} < \pi$. If it is steered to the direction θ_{s}, the beampattern should have N nulls, which satisfy $\theta_{\mathrm{s}} < \theta_{\mathrm{s}} + \theta_{N,1} < \cdots < \theta_{\mathrm{s}} + \theta_{N,N} < \theta_{\mathrm{s}} + \pi$. According to the symmetry requirement, the beampattern should also have N nulls that satisfy $\theta_{\mathrm{s}} - \pi < \theta_{\mathrm{s}} - \theta_{N,N} < \cdots < \theta_{\mathrm{s}} - \theta_{N,1} < \theta_{\mathrm{s}}$. As a result, the following symmetry constraints should be added to the beampattern:

$$\begin{aligned}
&\mathcal{B}\left[\mathbf{h}\left(\omega\right), \theta_{\mathrm{s}} + \theta_{N,n}\right] = \mathbf{d}^H\left(\omega, \theta_{\mathrm{s}} + \theta_{N,n}\right)\mathbf{h}\left(\omega\right) = 0,\\
&\mathcal{B}\left[\mathbf{h}\left(\omega\right), \theta_{\mathrm{s}} - \theta_{N,n}\right] = \mathbf{d}^H\left(\omega, \theta_{\mathrm{s}} - \theta_{N,n}\right)\mathbf{h}\left(\omega\right) = 0.
\end{aligned} \tag{19}$$

Combining the null constraints, the symmetry constraints due to the use of UCAs, and the distortionless constraint together, we get the following linear system of equations:

$$\mathbf{D}_{\mathrm{S}}\left(\omega\right)\mathbf{h}\left(\omega\right) = \mathbf{i}_{2N+1}, \tag{20}$$

where

$$\mathbf{D}_{\mathrm{S}}\left(\omega\right) = \begin{bmatrix} \mathbf{d}^H\left(\omega, \theta_{\mathrm{s}}\right) \\ \mathbf{d}^H\left(\omega, \theta_{\mathrm{s}} + \theta_{N,1}\right) \\ \mathbf{d}^H\left(\omega, \theta_{\mathrm{s}} - \theta_{N,1}\right) \\ \vdots \\ \mathbf{d}^H\left(\omega, \theta_{\mathrm{s}} + \theta_{N,N}\right) \\ \mathbf{d}^H\left(\omega, \theta_{\mathrm{s}} - \theta_{N,N}\right) \end{bmatrix} \tag{21}$$

is a matrix of size $(2N+1) \times M$, and $\mathbf{i}_{2N+1}$ is a vector of length $2N+1$, whose first element is 1 and all its other components are 0.

It can be readily checked that we need $M \geq 2N+1$ microphones to design a steerable Nth-order differential beamformer. This is consistent with the conclusion in (Huang *et al.*, 2017b) that at least $M = 2N+1$ microphones are needed for designing a continuously steerable differential beamformer. When $M = 2N+1$, the solution of (20) is

$$\mathbf{h}\left(\omega\right) = \mathbf{D}_{\mathrm{S}}^{-1}\left(\omega\right)\mathbf{i}_{2N+1}. \tag{22}$$

When $M > 2N+1$, the beamformer can be derived by maximizing the WNG, i.e.,

$$\begin{cases} \min \mathbf{h}^H\left(\omega\right)\mathbf{h}\left(\omega\right) \\ \text{s. t. } \mathbf{D}_{\mathrm{S}}\left(\omega\right)\mathbf{h}\left(\omega\right) = \mathbf{i}_{2N+1} \end{cases}. \tag{23}$$

The solution of (23) is then

$$\mathbf{h}_{\mathrm{MWNG}}\left(\omega\right) = \mathbf{D}_{\mathrm{S}}^H\left(\omega\right)\left[\mathbf{D}_{\mathrm{S}}\left(\omega\right)\mathbf{D}_{\mathrm{S}}^H\left(\omega\right)\right]^{-1}\mathbf{i}_{2N+1}. \tag{24}$$

Let us consider a design example. We have a UCA with $M = 8$ and $r = 2$ cm and we want design a 2nd-order hypercardioid differential beamformer with two

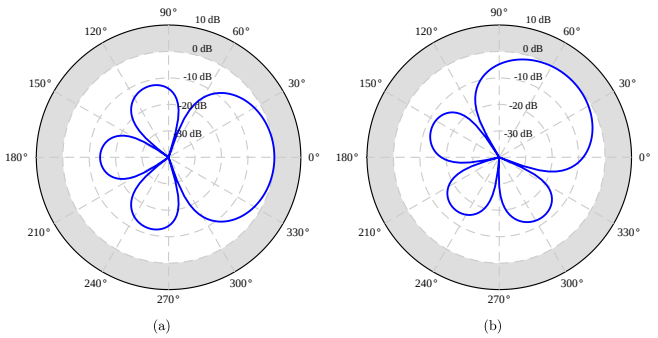

FIG. 3. Beampatterns of the differential beamformer designed with a UCA using symmetrical null constraints: (a) $\theta_{\mathrm{s}} = 0^\circ$ and (b) $\theta_{\mathrm{s}} = 50^\circ$. Conditions: $M = 8$, $r = 2.0$ cm, and $f = 1$ kHz.

nulls. When $\theta_{\mathrm{s}} = 0^\circ$, the two nulls are at 72° and 144°. When $\theta_{\mathrm{s}} = 50^\circ$, the two nulls are at 122° and 194°. Given these conditions, we designed the 2nd-order differential beamformer with the MWNG method in (24). Figure 3 plots the resulting beampatterns, which are identical at $\theta_{\mathrm{s}} = 0^\circ$ and $\theta_{\mathrm{s}} = 50^\circ$, and all the nulls appear in the expected directions, indicating that the method has successfully designed a fully steerable differential beamformer. As seen, the proposed method takes the same null constraints as the conventional method but this extension leads to a new way to design continuously steerable differential beamformers. Note that here "steerable" means that the beampattern pointing to the direction θ_{s} is simply a rotation of the beampattern pointing to 0°. The beamforming coefficients may need to be recomputed for different steering angle, which is slightly different from the conventional concept of "steerable."

Now, we consider the general case where some nulls are in the same direction, i.e., nulls with multiplicity greater than 1. Without loss of generality, we consider to design an Nth-order differential beamformer with N nulls but there is one null at $\theta_{N,n}$ with a multiplicity of Q $(1 \leq Q \leq N)$. Then, the directivity pattern with $\theta_{\mathrm{s}} = 0$ can be expressed as

$$\mathcal{B}_N\left(\theta\right) = \mathcal{B}_{N-Q}\left(\theta\right) \times \left(\cos\theta - \cos\theta_{N,n}\right)^Q, \tag{25}$$

where $\mathcal{B}_{N-Q}\left(\theta\right)$ is the directivity pattern corresponding to the other $N-Q$ nulls. It is easy to check that the qth (for $q = 1, 2, \ldots, Q-1$) derivative of $\mathcal{B}_N\left(\theta\right)$ with respect to $\cos\theta$ at $\cos\theta_{N,n}$ satisfies

$$\left.\frac{\partial^q \mathcal{B}_N\left(\theta\right)}{\partial(\cos\theta)^q}\right|_{\cos\theta=\cos\theta_{N,n}} = 0. \tag{26}$$

Consequently, the qth-order partial derivative of the beamformer's beampattern with respect to $\cos\theta$ at $\cos\theta_{N,n}$ should also satisfy (Chen *et al.*, 2014)

$$\left.\frac{\partial^q \mathcal{B}\left[\mathbf{h}\left(\omega\right), \theta\right]}{\partial(\cos\theta)^q}\right|_{\cos\theta=\cos\theta_{N,n}} = 0. \tag{27}$$

The previous expression is equivalent to

$$\left[\mathbf{d}^H(\omega,\theta_{N,n})\right]^{(q)}\mathbf{h}(\omega)=0, \tag{28}$$

for $q=1,2,\ldots,Q-1$, where

$$\left[\mathbf{d}^H(\omega,\theta_{N,n})\right]^{(q)}=\left.\frac{\partial^q\mathbf{d}^H(\omega,\theta)}{\partial(\cos\theta)^q}\right|_{\cos\theta=\cos\theta_{N,n}} \tag{29}$$

is the qth-order partial derivative of $\mathbf{d}^H(\omega,\theta)$ at $\cos\theta_{N,n}$. As shown in Appendix A, the mth element of the first, second, and third-order partial derivatives of $\mathbf{d}^H(\omega,\theta)$ are

$$\left[\frac{\partial\mathbf{d}^H(\omega,\theta)}{\partial(\cos\theta)}\right]_m=\left(\cos\psi_m-\frac{\cos\theta}{\sin\theta}\sin\psi_m\right)\times-\jmath\varpi e^{-\jmath\varpi\cos(\theta-\psi_m)}, \tag{30}$$

$$\left[\frac{\partial^2\mathbf{d}^H(\omega,\theta)}{\partial(\cos\theta)^2}\right]_m=\left[\left(\frac{1}{\sin\theta}+\frac{\cos^3\theta}{\sin^3\theta}\right)\sin\psi_m+\jmath\varpi\left(\cos\psi_m-\frac{\cos\theta}{\sin\theta}\sin\psi_m\right)^2\right]\times\jmath\varpi e^{-\jmath\varpi\cos(\theta-\psi_m)}, \tag{31}$$

$$\left[\frac{\partial^3\mathbf{d}^H(\omega,\theta)}{\partial(\cos\theta)^3}\right]_m=\left[\left(\frac{3\cos\theta}{\sin^3\theta}+\frac{3\cos^3\theta}{\sin^5\theta}\right)\sin\psi_m-3\jmath\varpi\left(\cos\psi_m-\frac{\cos\theta}{\sin\theta}\sin\psi_m\right)\times\left(\frac{1}{\sin\theta}+\frac{\cos^2\theta}{\sin^3\theta}\right)\sin\psi_m+(\jmath\varpi)^2\left(\cos\psi_m-\frac{\cos\theta}{\sin\theta}\sin\psi_m\right)^3\right]\times\jmath\varpi e^{-\jmath\varpi\cos(\theta-\psi_m)}. \tag{32}$$

Now, the constraints corresponding to the null $\theta_{N,n}$ (with multiplicity Q) for any steering direction θ_{s} become

$$\begin{aligned}\left[\mathbf{d}^H(\omega,\theta_{\mathrm{s}}+\theta_{N,n})\right]^{(q)}\mathbf{h}(\omega)=0,\\ \left[\mathbf{d}^H(\omega,\theta_{\mathrm{s}}-\theta_{N,n})\right]^{(q)}\mathbf{h}(\omega)=0,\end{aligned} \tag{33}$$

for $q=0,1,\ldots,Q-1$.

A special case is that the Nth-order differential beamformer has a null at the opposite direction of the desired direction, i.e., at $\theta_{\mathrm{s}}+\pi$, which can be either a single null or a null with multiplicity greater than 1. In this case, the constraints at $\theta_{\mathrm{s}}+\pi$ and $\theta_{\mathrm{s}}-\pi$ are essentially the same, so we only need the constraint at $\theta_{\mathrm{s}}+\pi$. For example, to design an Nth-order differential beamformer with a multiple null of order N at $\theta_{\mathrm{s}}+\pi$, the constraints matrix $\mathbf{D}_{\mathrm{S}}(\omega)$ should be

$$\mathbf{D}_{\mathrm{S}}(\omega)=\begin{bmatrix}\mathbf{d}^H(\omega,\theta_{\mathrm{s}})\\ \mathbf{d}^H(\omega,\theta_{\mathrm{s}}+\theta_{N,1})\\ \left[\mathbf{d}^H(\omega,\theta_{\mathrm{s}}+\theta_{N,2})\right]^{(1)}\\ \vdots\\ \left[\mathbf{d}^H(\omega,\theta_{\mathrm{s}}+\theta_{N,N})\right]^{(N-1)}\end{bmatrix}. \tag{34}$$

In a similar way, the corresponding filter can be computed with (22) or (24).

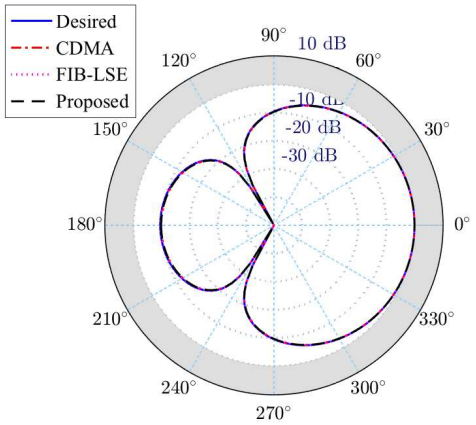

FIG. 4. The desired target beampattern and the beampatterns of the 1st-order differential beamformers designed with a UCA at $\theta_{\mathrm{s}}=0°$. Note that the beampatterns designed with all studied methods are identical to the target directivity pattern (the four lines coincide). Conditions: $M=8$, $r=2.0$ cm, and $f=1$ kHz

V. SIMULATIONS

We consider a UCA, of radius $r=2.0$ cm, consisting of 8 omnidirectional microphones. The desired target beampattern is the hypercardioid (Benesty and Chen, 2012; Elko, 2000), where the parameters of the 1st-, 2nd-, and 3rd-order hypercardioids ($\theta_{\mathrm{s}}=0°$) are listed in Table I. Note that the developed method does not need the knowledge of the target beampattern; the reason that we choose a target beampattern is to validate the feasibility and demonstrate the effectiveness of the method. For the purpose of comparison, we also show the results of the conventional null-constrained method, i.e., the method to design circular differential microphone arrays (CDMAs) (Benesty *et al.*, 2015) and the frequency-invariant beamformer deduced from the optimal approximation of the beampattern from a least-square error (LSE) perspective (FIB-LSE) (Huang *et al.*, 2017b).

In the first simulation, we design the 1st-order hypercardioid differential beamformer with one null. When $\theta_{\mathrm{s}}=0°$, the null is at 120°. The desired beampattern and the beampatterns of the beamformers designed with the

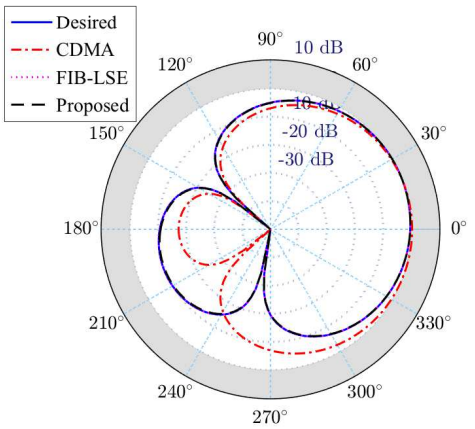

FIG. 5. The desired target beampattern and the beampatterns of the 1st-order differential beamformers designed with a UCA at $\theta_s = 20°$. The FIB-LSE and proposed methods successfully form the desired target beampattern (the three lines coincide), the CDMA method fails to form the desired beampattern. Conditions: $M = 8$, $r = 2.0$ cm, and $f = 1$ kHz.

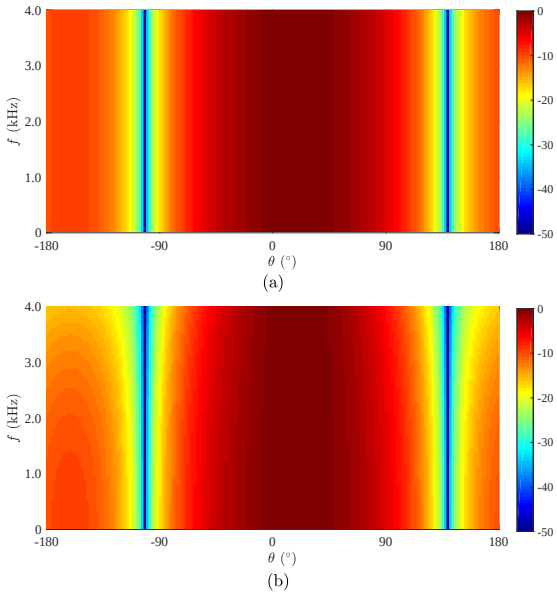

FIG. 6. A top view of the beampatterns versus frequency of the 1st-order differential beamformers designed with a UCA at $\theta_s = 20°$: (a) FIB-LSE method and (b) proposed method. The beampattern designed with the FIB-LSE method and the proposed method are almost frequency invariant. Conditions: $M = 8$ and $r = 2.0$ cm.

studied methods (at $f = 1$ kHz) are shown in Fig. 4. It is seen that the beampatterns designed with both the proposed method and conventional methods are identical to the target directivity pattern. When $\theta_s = 20°$, the null is at 140°. The target beampattern and the beampatterns of the beamformers designed with the studied methods

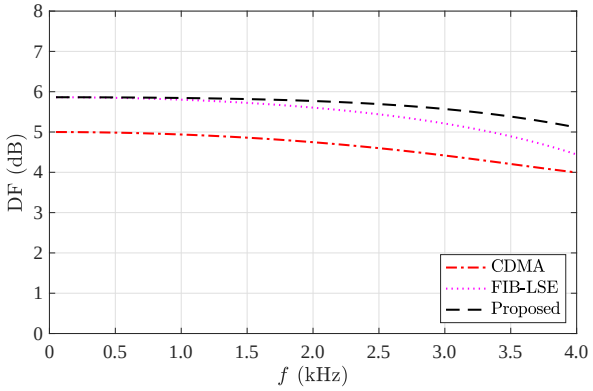

FIG. 7. DF of the 1st-order differential beamformers designed with a UCA at $\theta_s = 20°$. Conditions: $M = 8$ and $r = 2.0$ cm.

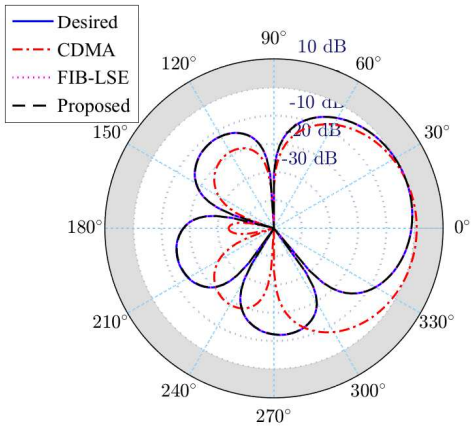

FIG. 8. The desired beampattern and beampatterns of the 2nd-order differential beamformers designed with a UCA at $\theta_s = 20°$. The FIB-LSE and proposed methods successfully form the desired beampattern (the three lines coincide), the CDMA method fails to form the desired beampattern. Conditions: $M = 8$, $r = 2.0$ cm, and $f = 1$ kHz.

(at $f = 1$ kHz) are shown in Fig. 5. It is seen that the beampattern designed with the FIB-LSE method and the proposed method are identical to the target directivity pattern. In contrast, the beampattern designed with the CDMA method is significantly different from the target beampattern. While it has nulls and unit gain at the specified directions, the beampattern's gain exceeds 1 in many other directions. It is also seen from Fig. 6 that the beampattern of the beamformer designed with the FIB-LSE method and the proposed method is nearly frequency invariant. We also study their DFs, the results are plotted in Fig. 7; it is seen that the proposed method achieved a DF value that is almost the same as that of the target directivity pattern, and is slightly higher than the FIB-LSE method and approximately 3 dB higher than that of the CDMA method.

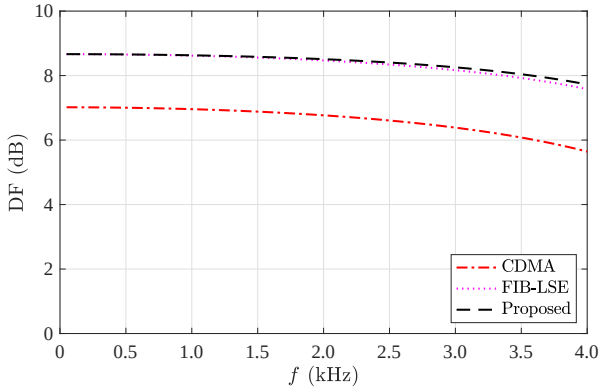

FIG. 9. DF of the 2nd-order differential beamformers designed with a UCA at $\theta_s = 20°$. Conditions: $M = 8$ and $r = 2.0$ cm.

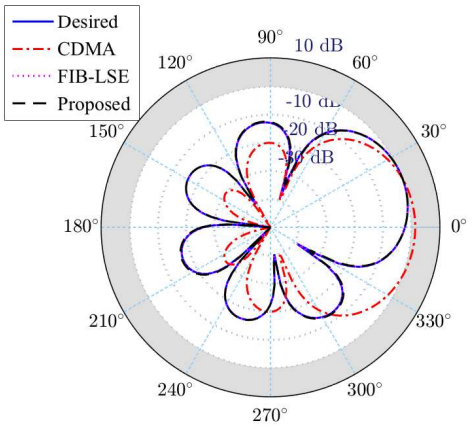

FIG. 10. Desired beampattern and designed beampatterns of the 3rd-order differential beamformers designed with a UCA at $\theta_s = 20°$. The FIB-LSE and proposed methods successfully form the desired beampattern (the three lines coincide), the CDMA method fails to form the desired beampattern. Conditions: $M = 8$, $r = 2.0$ cm, and $f = 1$ kHz.

In the second simulation, we design the 2nd-order hypercardioid differential beamformers with two nulls. When $\theta_s = 20°$, the two nulls are at 92° and 164°. Figure 8 plots the desired target beampattern and the beampatterns of the beamformers designed with the studied methods. It is seen that the FIB-LSE method and the proposed method successfully obtain the target beampattern. In comparison, the beampattern obtained using the CDMA method is very different from the desired target beampattern. Figure 9 plots the DFs of the differential beamformers. It is seen that the DF of the proposed beamformer is almost frequency invariant and approximately 2 dB higher than that of the CMDA method.

Next, we design the 3rd-order hypercardioid differential beamformers with three nulls. When $\theta_s = 20°$, the three nulls are at 71°, 123°, and 174°. The results are shown in Fig. 10. As seen, the beampattern designed using the CDMA method is distorted, while, again, the FIB-LSE and proposed methods work well.

TABLE I. Parameters of the 1st-, 2nd-, and 3rd-order hypercardioid ($\theta_s = 0°$).

1st-order	$\mathcal{B}_1(\theta) = \frac{1}{3} + \frac{2}{3}\cos\theta$ $\theta_{1,1} = 120°$
2nd-order	$\mathcal{B}_2(\theta) = \frac{1}{5} + \frac{2}{5}\cos\theta + \frac{2}{5}\cos(2\theta)$ $\theta_{2,1} = 72°$, $\theta_{2,2} = 144°$
3rd-order	$\mathcal{B}_3(\theta) = \frac{1}{7} + \frac{2}{7}\cos\theta + \frac{2}{7}\cos(2\theta) + \frac{2}{7}\cos(3\theta)$ $\theta_{3,1} = 51°$, $\theta_{3,1} = 103°$, $\theta_{3,1} = 154°$

Among the three compared methods, both the FIB-LSE and proposed methods successfully formed the target beampattern at different steering directions. The proposed method even exhibits slightly better frequency-invariant property than the FIB-LSE method. Moreover, the developed approach only requires to know the steering and nulls' directions instead of the exact target directivity pattern, which makes it more practical to use in real applications. In comparison, the beampattern of the CDMA method changes with the steering angle.

To demonstrate the steering flexibility of the proposed method, we plot in Fig. 11 the beampatterns of the 1st-, 2nd-, and 3rd-order hypercardioids designed with the developed null-constrained method at two steering directions of $\theta_s = 50°$ and $\theta_s = 120°$ (the target beampattern is the same as in the previous figures). One can see that the designed beampatterns are successfully steered to those directions. It should be noted that the choices of $\theta_s = 50°$ and $\theta_s = 120°$ are arbitrary and the same performance can be obtained with any steering angle.

Finally, we evaluate the steering error, which is defined as

$$\epsilon_{\mathcal{B}} = 10\log_{10}\int_0^{2\pi} \left|\mathcal{B}\left[\mathbf{h}\left(\omega\right),\theta\right] - \mathcal{B}_{N,\theta_s}(\theta)\right|^2 d\theta. \quad (35)$$

In the simulation, $\epsilon_{\mathcal{B}}$ is computed by dividing the range between 0 and 2π into 360 uniform parts and replacing the integral with the sum operation. Figure 12 plots the results. As seen, the steering error is very small and it does not change much with the steering angle for any given frequency.

VI. CONCLUSIONS

This paper studied the problem of differential beamforming with UCAs. By analyzing the properties of the circular array topology, we extended the null-constrained method that was previously developed for linear differential microphone arrays to the design of differential beamformers with circular microphone arrays. The prominent properties of this extended method include: 1) it can be used to design differential beamformers of any order and any shape of directivity pattern, with or without multiple

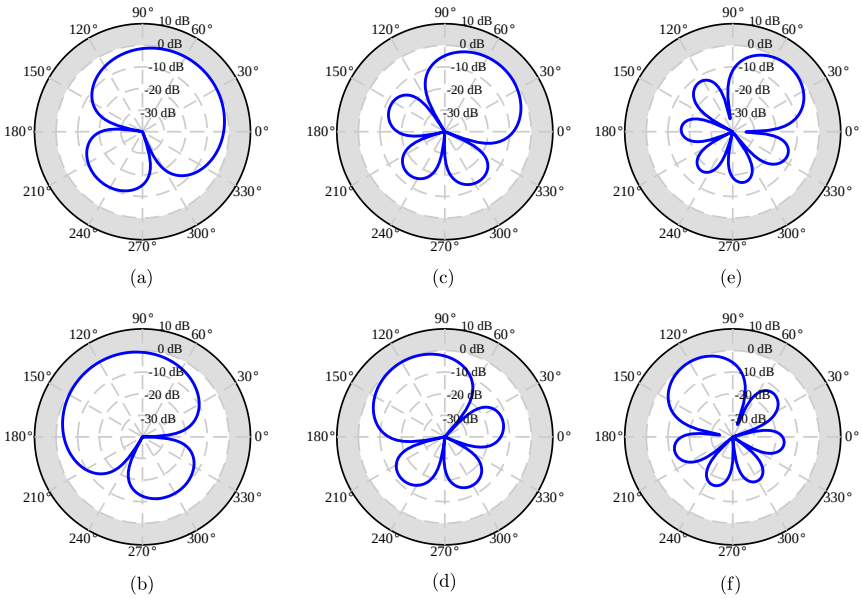

FIG. 11. Beampatterns of the proposed differential beamformers designed with a UCA for a steering direction: (a) 1st-order with $\theta_s = 50°$, (b) 1st-order with $\theta_s = 120°$, (c) 2nd-order with $\theta_s = 50°$, (d) 2nd-order with $\theta_s = 120°$, (e) 3rd-order with $\theta_s = 50°$, and (f) 3rd-order with $\theta_s = 120°$. Conditions: $M = 8$, $r = 2.0$ cm, and $f = 1$ kHz.

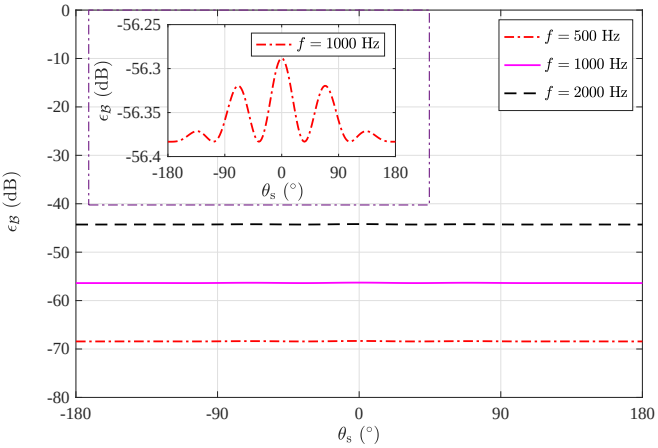

FIG. 12. Steering errors of the proposed differential beamformer designed with a UCA as a function of the steering direction. The dotted box is a zoomed plot for the steering error at $f = 1000$ Hz. Conditions: $M = 8$ and $r = 2.0$ cm.

nulls; 2) the differential beamformers designed with this extended method are fully steerable, i.e., the beampattern remains the same if steered to a different direction; and 3) the method only requires to know the steering angle and the directions of the nulls, and as a result it is efficient in practice.

ACKNOWLEDGMENTS

This research was supported by the Israel Science Foundation (grant no. 576/16) and the ISF-NSFC joint research program (grant No. 2514/17 and 61761146001).

APPENDIX:

The mth element of $\left[\mathbf{d}^H(\omega,\theta)\right]^{(q)}$, i.e, $f_m^{(q)}(\cos\theta)$, is

$$f_m^{(q)}(\cos\theta) = \frac{\partial^q\left[e^{-\jmath\varpi\cos(\theta-\psi_m)}\right]}{\partial(\cos\theta)^q} = \frac{\partial^q\left[e^{-\jmath\varpi(\cos\theta\cos\psi_m+\sin\theta\sin\psi_m)}\right]}{\partial(\cos\theta)^q}. \quad \text{(A.1)}$$

Setting $x = \cos\theta$, we have

$$f_m^{(q)}(x) = \frac{\partial^q\left[e^{-\jmath\varpi g(x)}\right]}{\partial x^q}, \quad \text{(A.2)}$$

where $g(x) = x\cos\psi_m + \sqrt{1-x^2}\sin\psi_m$. From (A.2), it is not difficult to check that

$$\begin{aligned} f_m^{(1)}(x) &= -\jmath\varpi g^{(1)}(x)\, e^{-\jmath\varpi g(x)} \\ f_m^{(2)}(x) &= \jmath\varpi e^{-\jmath\varpi g(x)}\left\{\jmath\varpi\left[g^{(1)}(x)\right]^2 - g^{(2)}(x)\right\} \\ f_m^{(3)}(x) &= \jmath\varpi e^{-\jmath\varpi g(x)}\left\{-g^{(3)}(x) + 3\jmath\varpi g^{(1)}(x)g^{(2)}(x) - (\jmath\varpi)^2\left[g^{(1)}(x)\right]^3\right\}. \end{aligned} \quad \text{(A.3)}$$

We have

$$
\begin{aligned}
g^{(1)}(x) &= \cos\psi_m - x(1-x^2)^{-\frac{1}{2}}\sin\psi_m \\
g^{(2)}(x) &= -\left[(1-x^2)^{-\frac{1}{2}} + x^2(1-x^2)^{-\frac{3}{2}}\right]\sin\psi_m \\
g^{(3)}(x) &= -\left[3x(1-x^2)^{-\frac{3}{2}} + 3x^3(1-x^2)^{-\frac{5}{2}}\right]\sin\psi_m.
\end{aligned} \tag{A.4}
$$

Substituting $x = \cos\theta$ into (A.4) gives

$$
\begin{aligned}
g^{(1)}(\cos\theta) &= \cos\psi_m - \frac{\cos\theta}{\sin\theta}\sin\psi_m \\
g^{(2)}(\cos\theta) &= -\left(\frac{1}{\sin\theta} + \frac{\cos^3\theta}{\sin^3\theta}\right)\sin\psi_m \\
g^{(3)}(\cos\theta) &= -\left(\frac{3\cos\theta}{\sin^3\theta} + \frac{3\cos^3\theta}{\sin^5\theta}\right)\sin\psi_m.
\end{aligned} \tag{A.5}
$$

Substituting (A.5) into (A.3), we obtain (30)–(32).

Benesty, J., and Chen, J. (**2012**). *Study and Design of Differential Microphone Arrays* (Berlin, Germany: Springer-Verlag).

Benesty, J., Chen, J., and Cohen, I. (**2015**). *Design of Circular Differential Microphone Arrays* (Berlin, Germany: Springer-Verlag).

Benesty, J., Cohen, I., and Chen, J. (**2017**). *Fundamentals of Signal Enhancement and Array Signal Processing* (John Wiley & Sons).

Bernardini, A., D. Aria, M., Sannino, R., and Sarti, A. (**2017**). "Efficient continuous beam steering for planar arrays of differential microphones," IEEE Signal Process. Lett. **24**(6), 794–798.

Bitzer, J., and Simmer, K. U. (**2001**). "Superdirective microphone arrays," in *Microphone Arrays* (Springer), pp. 19–38.

Borra, F., Bernardini, A., Antonacci, F., and Sarti, A. (**2019**). "Uniform linear arrays of first-order steerable differential microphones," IEEE/ACM Trans. Audio, Speech, Lang. Process. **27**(12), 1906–1918.

Borra, F., Bernardini, A., Antonacci, F., and Sarti, A. (**2020**). "Efficient implementations of first-order steerable differential microphone arrays with arbitrary planar geometry," IEEE/ACM Trans. Audio, Speech, Lang. Process. .

Bouchard, C., Havelock, D. I., and Bouchard, M. (**2009**). "Beamforming with microphone arrays for directional sources," J. Acoust. Soc. Am. **125**(4), 2098–2104.

Buchris, Y., Cohen, I., and Benesty, J. (**2019**). "On the design of time-domain differential microphone arrays," Applied Acoustics **148**, 212–222.

Buchris, Y., Cohen, I., Benesty, J., and Amar, A. (**2020**). "Joint sparse concentric array design for frequency and rotationally invariant beampattern," IEEE/ACM Trans. Audio, Speech, Lang. Process. **28**, 1143–1158.

Buck, M. (**2002**). "Aspects of first-order differential microphone arrays in the presence of sensor imperfections," European Trans. Telecomm. **13**(2), 115–122.

Byun, J., Park, Y. C., and Park, S. W. (**2018**). "Continuously steerable second-order differential microphone arrays," J. Acoust. Soc. Am. **143**(3), EL225–EL230.

Chen, J., Benesty, J., and Pan, C. (**2014**). "On the design and implementation of linear differential microphone arrays," J. Acoust. Soc. Am. **136**, 3097–3113.

Crocco, M., and Trucco, A. (**2010**). "The synthesis of robust broadband beamformers for equally-spaced linear arrays," J. Acoust. Soc. Am. **128**(2), 691–701.

Elko, G. W. (**1996**). "Microphone array systems for hands-free telecommunication," Speech Commun. **20**(3), 229–240.

Elko, G. W. (**2000**). "Superdirectional microphone arrays," in *Acoustic Signal Processing for Telecommunication* (Springer), pp. 181–237.

Elko, G. W. (**2004**). "Differential microphone arrays," in *Audio Signal Processing for Next-Generation Multimedia Communication Systems* (Springer), pp. 11–65.

Elko, G. W., and Meyer, J. (**2008**). "Microphone arrays," in *Springer Handbook of Speech Processing*, edited by J. Benesty, M. M. Sondhi, and Y. Huang (Berlin, Germany: Springer-Verlag), Chap. 48, pp. 1021–1041.

Elko, G. W., and Pong, A.-T. N. (**1997**). "A steerable and variable first-order differential microphone array," in *Proc. IEEE ICASSP*, IEEE, Vol. 1, pp. 223–226.

Gannot, S., Burshtein, D., and Weinstein, E. (**2004**). "Analysis of the power spectral deviation of the general transfer function GSC," IEEE Trans. Signal Process. **52**, 1115–1120.

Greene Jr, C. R., McLennan, M. W., Norman, R. G., McDonald, T. L., Jakubczak, R. S., and Richardson, W. J. (**2004**). "Directional frequency and recording (DIFAR) sensors in seafloor recorders to locate calling bowhead whales during their fall migration," J. Acoust. Soc. Am. **116**(2), 799–813.

Huang, G., Benesty, J., and Chen, J. (**2017**a). "Design of robust concentric circular differential microphone arrays," J. Acoust. Soc. Am. **141**(5), 3236–3249.

Huang, G., Benesty, J., and Chen, J. (**2017**b). "On the design of frequency-invariant beampatterns with uniform circular microphone arrays," IEEE/ACM Trans. Audio, Speech, Lang. Process. **25**(5), 1140–1153.

Huang, G., Benesty, J., Cohen, I., and Chen, J. (**2020**a). "Differential beamforming on graphs," IEEE/ACM Trans. Audio, Speech, Lang. Process. **28**(1), 901–913.

Huang, G., Benesty, J., Cohen, I., and Chen, J. (**2020**b). "A simple theory and new method of differential beamforming with uniform linear microphone arrays," IEEE/ACM Trans. Audio, Speech, Lang. Process. **28**(1), 1079–1093.

Huang, G., Chen, J., and Benesty, J. (**2018**). "On the design of differential beamformers with arbitrary planar microphone array," J. Acoust. Soc. Am. **144**(1), EL66–EL70.

Huang, G., Chen, J., and Benesty, J. (**2019**). "Design of planar differential microphone arrays with fractional orders," IEEE/ACM Trans. Audio, Speech, Lang. Process. **28**, 116–130.

Kolundzija, M., Faller, C., and Vetterli, M. (**2011**). "Spatiotemporal gradient analysis of differential microphone arrays," Journal Audio Eng. Soc. **59**(1/2), 20–28.

Lovatello, J., Alberto, B., and Augusto, S. (**2018**). "Steerable circular differential microphone arrays," in *Proc. EUSIPCO*, IEEE, pp. 1245–1249.

Olson, H. F. (**1946**). "Gradient microphones," J. Acoust. Soc. Am. **17**(3), 192–198.

Schwartz, O., Gannot, S., and Habets, E. A. (**2017**). "Multispeaker LCMV beamformer and postfilter for source separation and noise reduction," IEEE/ACM Trans. Audio, Speech, Lang. Process. **25**(5), 940–951.

Yan, S. (**2015**). "Optimal design of modal beamformers for circular arrays," J. Acoust. Soc. Am. **138**(4), 2140–2151.

Yan, S., Ma, Y., and Hou, C. (**2007**). "Optimal array pattern synthesis for broadband arrays," J. Acoust. Soc. Am. **122**(5), 2686–2696.

Yan, S., Sun, H., Ma, X., Svensson, U. P., and Hou, C. (**2011**). "Time-domain implementation of broadband beamformer in spherical harmonics domain," IEEE Trans. Acoust., Speech, Signal Process. **19**, 1221–1230.